ACS ORGANIC & INORGANIC Au
AN OPEN ACCESS JOURNAL OF THE AMERICAN CHEMICAL SOCIETY

pubs.acs.org/orginorgau

Article

Boosting Gold(I) Catalysis via Weak Interactions: New Fine-Tunable Impy Ligands

Riccardo Pedrazzani, Angela Pintus, Roberta De Ventura, Marianna Marchini, Paola Ceroni, Carlos Silva López, Magda Monari,* and Marco Bandini*

Cite This: *ACS Org. Inorg. Au* 2022, 2, 229–235

Read Online

ACCESS | Metrics & More | Article Recommendations | Supporting Information

ABSTRACT: A series of modular ImPy–carbene–Au(I) complexes are synthesized and fully characterized both in the solid state and in solution. The presence of oligoaryl units (phenyl and thienyl rings) at the C5-position of the ImPy core (in close proximity to the gold center) imprints on the organometallic species fine-tunable and predictable catalytic properties. A marked accelerating effect was recorded in several [Au(I)]-catalyzed electrophilic activations of unsaturated hydrocarbons when a CF_3-containing aromatic ring was accommodated at the ImPy core.

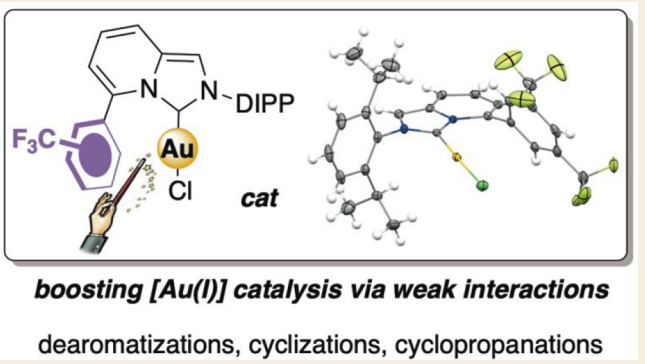

KEYWORDS: *carbene ligands, fine-tunability gold, homogeneous catalysis, secondary interactions*

Homogenous gold catalysis has rapidly emerged as an established tool in synthetic organic methodologies.[1−4] Despite its relatively young age (pioneering studies date back to early 2000), the use of gold(I) species in the electrophilic activation of unsaturated hydrocarbons and cross-coupling reactions has already begun to parallel the use of longer investigated and more consolidated noble metal catalysis. The robustness and adaptability of gold(I) catalysis in multifaceted applications is witnessed daily by its exploitation to enable synthetic methodologies such as photocatalysis, the total synthesis of structurally elaborated bioactive and photoactive molecular motifs, asymmetric catalysis, dual catalysis, electrosynthesis, and flow-chemistry.[5−8] This scenario is the consequence of the ongoing request for dedicated gold complexes featuring a predesigned flexible and fine-tunable catalytic performance.[9] Among others, the use of readily available *N*-heterocyclic carbenes (NHCs)[10−13] as ligands in gold chemistry[14−18] deserves a particular mention due to the strong σ-donating properties of the soft singlet carbon atom of NHCs, which results in Au complexes (soft metal) commonly featuring high stabilities and yet unique catalytic activities.[19,20] Additionally, NHCs can rapidly access impressive organometallic diversity and complexity by incorporating a theoretically unlimited range of functionalities, a key requisite for the development of "on-demand" catalysts. In this wide and dynamic picture, the development of unsymmetrically substituted monodentate NHC ligands is receiving growing credit due to its prompt access to unlimited fine-tunable gold species and modular stereochemical environments for asymmetric transformations.[21−23]

The robust and readily accessible imidazo[1,5-*a*]pyridin-3-ylidene platform (ImPy) **A** (introduced almost simultaneously by Lassaletta[24] and Glorius[25]) covers a prominent role in metal–carbene chemistry,[26−33] allowing the installation of steric as well as electronic tools in close proximity to the metal center (i.e., C5-position of the ImPy core). In addition, ImPy shows a higher oxidation resistance and better synthetic accessibility with respect to P-based analogous ligands (Figure 1, top). As a consequence, over the past years fully characterized [Au(I)]- and [Au(III)]–ImPy complexes[34−36] have been documented with ultimate applications in metal drug chemistry[37] and catalysis.[38−41] Modulating effects through steric constraints at the C5-position have been extensively investigated; however, the overall impact of electronic parameters have been far less systematically accounted so far and has been limited to the introduction of electron-rich aromatic pendants.[42]

In the present work, a systematic investigation on a new family of C5-oligoaryl-ImPy gold complexes was carried out,

Received: November 29, 2021
Revised: December 21, 2021
Accepted: December 22, 2021
Published: January 13, 2022

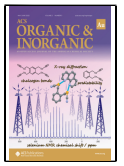

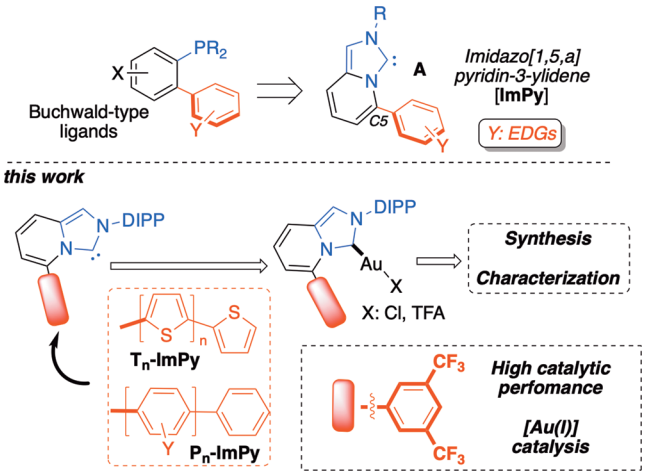

Figure 1. Chemical engineerization of fine-tunable C5-oligoaryl–ImPy gold complexes (DIPP, 2,5-diisopropyl-phenyl).

disclosing an unprecedented role of the electron-deficient 3,5-$(CF_3)_2$-phenyl ring in modulating and enhancing the catalytic activity of cationic gold(I) complexes in several transformations involving carbocationic- or carbene-like organogold intermediates (Figure 1, bottom).[19]

In line with our ongoing interest in homogeneous gold catalysis[43−50] and fine-tunable organometallic adducts via "secondary interactions",[51−56] we describe here two series of C5-oligoaryl imidazolium salts **6a−g**, featuring phenyl- (P_n-ImPy) and 2-thienyl- (T_n-ImPy) based pendants (Scheme 1). The role of the electronic properties imprinted by the diversely functionalized π-clouds on the P_n-ImPy and T_n-ImPy carbene series was assessed in three different gold-catalyzed methodologies by a combined SC-XRD and DFT investigation of the corresponding [Au(I)] complexes.[57,58]

Imidazopyridinium salts were obtained via initial Suzuki–Miyaura cross-coupling reactions among the pyridyl aldehyde **1** and the corresponding aryl-boronic acids **2a−f**. The 6-aryl pyridylcarbaldehydes **3** were isolated in excellent yields (65–98%) under optimal conditions (Scheme 1a). Then, the corresponding imines **5** were obtained quantitatively under dehydrative conditions ($MgSO_4$, Et_2O, rt) in the presence of 2,6-$(iPr)_2$-aniline **4** (Scheme 1b). Finally, the desired imidazolium platforms **6a−f** were achieved via a ring-closing strategy in the presence of $(CH_2O)_n$ and TMSX (X = Br, Cl; 74–94%, Scheme 1c). Differently, for the synthesis of the T3-ImPy·HBr **6g**, a Pd(0)-catalyzed Suzuki–Miyaura coupling between the Br derivative **7**[40] and the commercially available terthienyl-boronate **8** (69%) was adopted.

Subsequently, the C(5)-substituted imidazo[1,5-*a*]-pyridinium halides **6a−g** were subjected to the [Au(I)] complexation (**10a−g**) *via* metal metathesis through the corresponding Ag-complexes (**9**). The protocol (DCM, rt, dark, 16 h) proved highly competent in all cases, yielding the desired air-stable LAuCl complexes in excellent overall yields (81–99%, Scheme 2).

Scheme 1. Synthetic Sequence for the Preparation of P_n- and T_n-ImPy·HX 6a−g

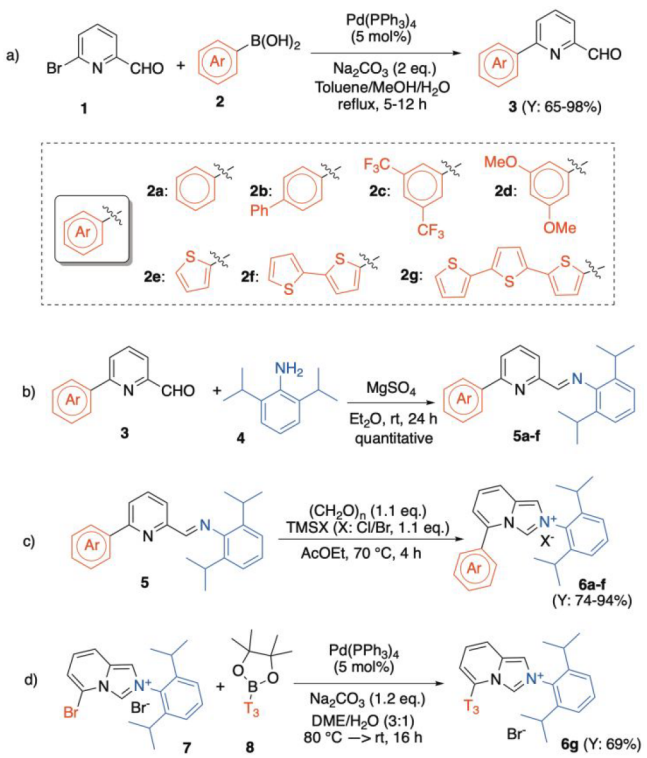

Scheme 2. Two-Step Procedure for the Synthesis of T_n- or P_nImPy–AuCl complexes 10a−g *via* a Metal Exchange Protocol of the Silver Analogues 9

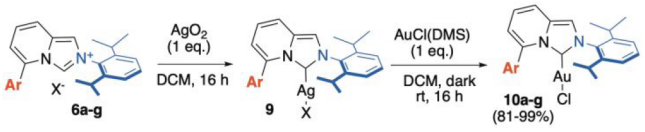

Some of us has recently documented the combined role of the cationic [Au(I)] center and basic anions[59,60] in the chemo-, regio-, and stereoselective dearomatization of 2-naphthols[61−67] with allenamides,[68−70] discovering the synergistic role of multiple secondary interactions in controlling the mechanistic profile.[71,72] In this line, we elected the dearomative process of dimethyl-naphthol **12** and allenamide **13** (Scheme 3) as a model control experiment for testing new [ImPyAuCl] complexes **10a−g**.[73] For these experiments, the corresponding trifluoroacetate complexes **11a−g** were generated *in situ* via a chloride scavenging reaction of complexes

Scheme 3. P_n-ImPy–AuCl/AgTFA- and T_n-ImPy–AuCl/AgTFA-Catalyzed Dearomatization of Naphthol 12[a]

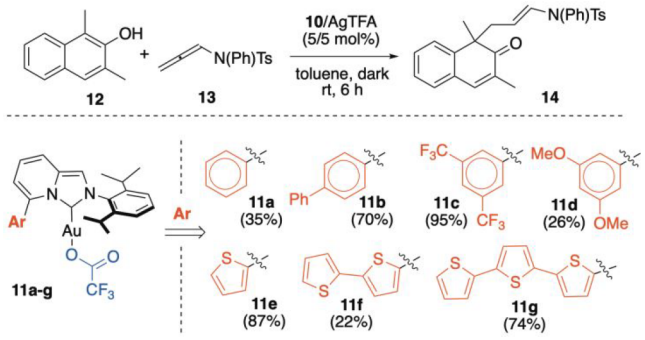

[a]The yields are reported as an average of two runs.

https://doi.org/10.1021/acsorginorgau.1c00052
ACS Org. Inorg. Au 2022, 2, 229−235

10 with AgTFA. The catalytic performances of the NHC−gold complexes are summarized in Scheme 3.

From the data collected in the Scheme 3, several interesting conclusions can be drawn. The P_n-ImPyAuCl series provided product **14** from very low to almost quantitative yields (26−95%) with an unexpected correlation to the electronic properties of the pendant group at C5. As a matter of fact, while electron-rich pendants are generally accommodated in the organic ligand to stabilize cationic Au(I) intermediates via stacking interactions,[74] in our case the incorporation of the 3,5-$(CF_3)_2$-C_6H_3 unit (**11c**) resulted as the best catalyst, providing **14** in a 95% yield.

Furthermore, complex **11c** showed the highest initial reaction rate among the complexes tested (**11a−11d**); more precisely, the rate was ca. 2.8× higher than that of the 3,5-$(OMe)_2$Ph-containing NHC−[Au(I)] complex **11d** (see the SI for details).

To shed light on this intriguing and unexpected chemical outcome, a dedicated crystallographic investigation was carried out on both series of P_n- and T_n-ImPy−AuCl complexes. Suitable single crystals for the SC-XRD analysis of complexes **10a−g** were obtained via vapor diffusion of *n*-hexane in DCM/toluene solutions of gold adducts. Some representative X-ray structures are depicted in Figure 2 (see the SI for further details).

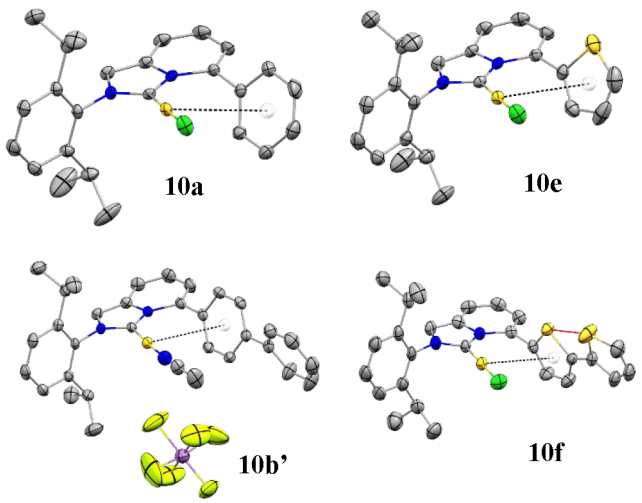

Figure 2. Representative molecular structures for complexes **10a**, **10e**, **10b′**, and **10f**. Hydrogen atoms were removed for clarity. The $Ar_{centroid}$···Au interaction is shown as black dashed lines. The S_1···S_2 interaction (**10f**) is shown as a red line.

All synthesized [Au(I)] complexes showed a linear bicoordination geometry with the Cl atom *trans* to the NHC ligand and an almost perpendicular orientation of the bulky DIPP unit with respect to the imidazolyl ring (dihedral angles range from 83.84° to 87.79°, Table S11). This common arrangement is a consequence of the rotational restriction faced by the 2,6-diisopropyl substituents. Additionally, intramolecular Au···π contacts with the aryl pendants at the C5-position were observed.

In line also with recent findings by Toste and Sigman,[75] who elegantly disclosed strong structure−catalytic activity correlations in regio-divergent [Au(I)]-catalyzed cycloaddition reactions, we targeted Au−Cl, Au−C1, and Au···Ar crystallographic distances as potential probe parameters to indirectly predict or rationalize the catalytic performances of the new ImPy−AuCl complexes. In this study, the cationic [**10b**−Au(CH_3CN)](SbF_6) complex **10b′** (Figure 2) was also taken into account, comparing the influence of the cationic metal center on the crystallographic data.

In Table 1, several structural parameters have been collected for a simplified comparative analysis.

Table 1. Structural Parameters Obtained by SC-XRD for ImPy−AuCl Complexes 10

10	Au−Cl (Å)	Au−C1 (Å)	Au···Ar (Å)[a]	Ar−ImPy (°)[b]
10a	2.304(3)	1.983(7)	3.511	56.95
10b	2.2828(9)	1.985(3)	3.412	67.65
10b'	2.019(3)b	1.974(3)	3.384	61.62
10c	2.287(1)	1.982(5)	3.352	64.63
10d	2.2765(9)	1.980(2)	3.353	64.94
10e	2.277(2)	1.981(7)	3.526	57.52
10f	2.267(2)	1.983(6)	3.477	82.58
10g	2.2932(6)	1.970(3)	3.456	73.20

[a]The distance between [Au(I)] and the center of mass of the aromatic ring at C5, as calculated by Mercury. [b]The Au−N(ACN) distance.

Interestingly, the Au−C1 distances were scarcely affected by the electronic properties of the ligand (Au−C1 range of 1.970−1.983 Å). The truncated conjugation at C5 between the ImPy core and the aryl ring could be responsible for this trend. The large dihedral angles recorded in the solid state for the two aromatic systems (Ar and ImPy, 56.95−82.58°) are in good agreement with this hypothesis. Similarly, the Au−Cl distances (2.267−2.304 Å) showed only slight variations. In particular, while almost constant Au−Cl distances were observed in the P_n-ImPyAuCl series (**10a−d**), the T_n-ImPyAuCl family shows shorter distances for mono- and bithienyl substituents (**10e** and **10f**) but a longer distance in the case of the *tert*-thienyl pendant (**10g**).

Therefore, Au···Ar contacts were examined across the two series P_n and T_n. First, by increasing the number of aryl units in both series, closer intramolecular contacts were identified. This trend nicely correlates with the electron-richness of oligoaryl cores that increases along with the number of repeating units. Second, a comparison between the **10b′** and **10b** (entries 2 and 3, Table 1) revealed only a slight contraction in both the C1−Au bond and the Au···Ar contact for the cationic complex, supporting the suitability of the Au−Cl precursors **10a−g** for the structure−activity relationship investigation. Interestingly, the introduction of arenes featuring opposite electronic properties such as 3,5-$(OMe)_2$-Ph (**10d**) and 3,5-$(CF_3)_2$-Ph (**10c**) caused a shortening of the Au···Ar distances (3.353−3.352 Å) in both cases with respect to unsubstituted **10a** (3.511 Å). However, a drastic change in the catalytic outcome was highlighted in the **10a−c** series (95% yield with **10c** and 26% yield with **10d**).

Concerning the T_n-ImPyAuCl series, no direct S(thienyl)···Au contacts have emerged regardless the length of the oligothienyl.[49,76] Surprisingly, **10f** showed a quite uncommon *cis*-arrangement of the two thienyl sulfur atoms in the solid state (Figure 2, S1···S2 = 3.301 Å).[77] This feature can be attributed to the fact that the S1···S2 forces play a stabilizing role in the packing efficiency.[78] On the contrary, complex **10g** bearing a terthienyl chain at C5 shows the conventional *trans*-*trans*-arrangement of the thienyl units (see the SI). The

https://doi.org/10.1021/acsorginorgau.1c00052
ACS Org. Inorg. Au 2022, 2, 229−235

uncommon *cis*-arrangement observed for the **T2** side arm could be tentatively targeted to rationalize the unsatisfactory catalytic performance of **10f**–AgTFA (Y = 22%).[79] Differently, **T1** and **T3** bearing gold complexes worked smoothly in the dearomative process, delivering **14** in 87% and 74% yields, respectively. The slight drop in the chemical outcome for **10g** might be ascribed to the more electron-rich **T3** and consequent "shielding" of the electrophilic properties of [Au(I)] center (Au···Ar = 3.536 and 3.456 for **10e** and **10g**, respectively). Additionally, the photophysical properties of the T3-ImPy series (**6g** and **10g**) were investigated both in solution (DCM) and in solid state (see Figures S1 and S2 and Table S4). Here, a significant drop in the emission quantum yield of the **T3** salt **6g** (6.2%) was recorded when the metal center was introduced (0.2%, **10g**). This phenomenon could be tentatively assigned to a higher efficiency of the non-radiative intersystem crossing deactivation of the fluorescent excited state promoted by the heavy atom effect.

To further analyze the electronic nature of such Au···Ar interactions and to provide a visual representation of them, we resorted to electronic structure calculations using density functional theory on complexes **10a**, **10c**, and **10d**.[80,81] Geometry optimizations and a topological analysis of the obtained electron density was performed using the atoms in molecules (AIM) and non-covalent interactions (NCIs) models.[82,83] Calculations were performed at the B3LYP/6-31+G(d) level for main-group atoms, and the SDD basis set and electron core potential were used for the Au atom.[84,85] We resorted to this compact basis set due to the large size of the complexes and the previous systematic benchmark showing that this particular combination of density functional and basis set, although compact, was able to reproduce gold chemistry with a comparable accuracy to triple-ζ and even larger basis sets.[86,87] Actually, our calculations faithfully reproduced the experimentally recorded X-ray structures. Not only close steric contacts were observed from the NCIs analysis (Figure 3, right) but a full covalent bond-like topology was also detected under the AIM analysis. A bond critical point can be found between the gold atom and the aryl fragment, along with the expected ring critical point to fulfill the Poincaré–Hopf rule. Therefore, both analyses point toward intimate Au···aryl interactions in these complexes (Figure 3, left).

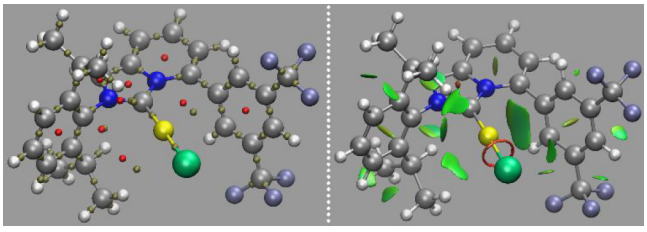

Figure 3. Ring and bond critical points of the electron density of **10c** (left) and the close noncovalent Au···π-aryl steric contact (right).

Further support for this interpretation was gathered via a population analysis of the electron density calculated for intermediate **A** when the aryl C5-pendant was undecorated and also when it was *meta*-disubstituted with CF_3 and OMe groups (Scheme 4). The partial charges found at the electrophilic end of the allenamide framework in these intermediates are fully compatible with the view of increased reactivity due to the electron-withdrawing effects of the C5-pendant when substituted with CF_3. Gratifyingly, charge values at this reactive terminus (0.037, 0.035, and 0.041 au for the –OMe-substituted, unsubstituted, and $-CF_3$-substituted systems, respectively) correlate well with the observed experimental yields.

Scheme 4. Proposed Reaction Intermediate A and Its Natural Bond Orbital (NBO) Partial Charge at the Electrophilic CH_2 Terminus with Respect to the C5-Pendant Substitution

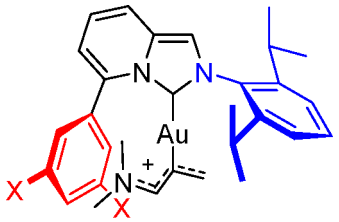

X	charge
CF_3	0.041
H	0.037
OMe	0.035

Intermediate A

In addition, the marked deviation from planarity recorded for the NHC and aryl skeletal unit (see Table 1) precludes a major impact of the arene electronic features on the whole ImPy carbene fragment and elects the Ar···[Au] secondary contacts as responsible for the fine-tuning of the catalytic performance.

Finally, we decided to assess the extensibility of this unprecedent accelerating effect of the CF_3-containg ring to other [Au(I)]-catalyzed manipulations of unsaturated hydrocarbons. In this regards, two chemical transformations based on carbocationic- or carbene-like organogold intermediates,[19] namely olefin cyclopropanation[88] and the cyclization of alkynylbenzaldehyde,[89] were analyzed (Scheme 5).

Scheme 5. Olefin Cyclopropanations and Alkynylbenzaldehyde Cyclizations: Examples of the Accelerating Effect of CF_3-Containing Carbene Ligands in [Au(I)] Catalysis

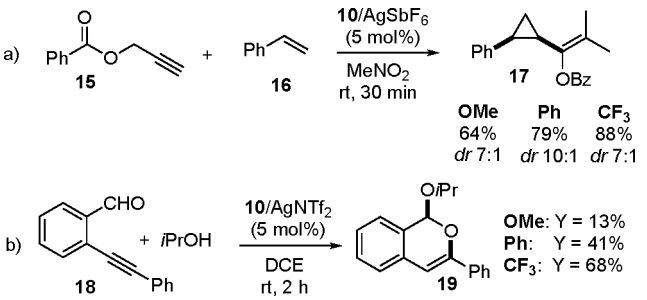

In this regard, the intermolecular olefin cyclopropanation introduced by Toste was first performed in the presence of complexes **10a,c–d**/$AgSbF_6$ (Scheme 5a). Interestingly, a marked increase of the chemical outcome toward the formation of the cyclopropane *cis*-**17** (yield up to 88%) was observed when fluorinated complex **10c** was adopted. The same trend was recorded also in the cyclization of the alkynylbenzaldehyde **18** in the presence of isopropanol. Here, **10c**/$AgNTf2_6$ (5 mol %) provided the acetal **19** in a 68% yield, more than fivefold that obtained with the electron-rich complex **10d** (Scheme 5b). Finally, it is worth mentioning that this reactivity trend was not affected by the loading of the gold complex. As a matter of fact, when catalysts **10** were

https://doi.org/10.1021/acsorginorgau.1c00052
ACS Org. Inorg. Au 2022, 2, 229–235

employed in a 2.5 mol % loading, a similar chemical outcome relationship was recorded.[90]

In conclusion, we have documented the preparation, characterization (spectroscopic and crystallographic), and use in catalysis of a new class of ImPyAuX complexes featuring diversely substituted aromatic pendants at the C5-position. The impact of electronically different side-arms on the overall catalytic properties of the gold complexes (*i.e.*, dearomatization of naphthols with allenamides) was examined through dedicated kinetic experiments, revealing an unusual accelerating action exerted by the 3,5-$(CF_3)_2$-Ph unit. Activating secondary interactions exerted by the ligand C5-pendant on the gold−alkylidene intermediate were accounted for the experimental outcome that resulted effective in several Au-mediated electrophilic activations of unsaturated hydrocarbons.

■ ASSOCIATED CONTENT

Supporting Information

The Supporting Information is available free of charge at https://pubs.acs.org/doi/10.1021/acsorginorgau.1c00052.

General synthetic procedures; photophysical, crystallographic, and computational data; and NMR spectra (PDF)

Accession Codes

CCDC 2091513−2091520 contain the supplementary crystallographic data for this paper. These data can be obtained free of charge via www.ccdc.cam.ac.uk/data_request/cif, or by emailing data_request@ccdc.cam.ac.uk, or by contacting The Cambridge Crystallographic Data Centre, 12 Union Road, Cambridge CB2 1EZ, UK; fax: +44 1223 336033.

■ AUTHOR INFORMATION

Corresponding Authors

Marco Bandini − *Dipartimento di Chimica "Giacomo Ciamician", Alma Mater Studiorum, 40126 Bologna, Italy; Center for Chemical Catalysis—C3, 40126 Bologna, Italy;* orcid.org/0000-0001-9586-3295; Email: marco.bandini@unibo.it

Magda Monari − *Dipartimento di Chimica "Giacomo Ciamician", Alma Mater Studiorum, 40126 Bologna, Italy;* Email: magda.monari@unibo.it

Authors

Riccardo Pedrazzani − *Dipartimento di Chimica "Giacomo Ciamician", Alma Mater Studiorum, 40126 Bologna, Italy*

Angela Pintus − *Dipartimento di Chimica "Giacomo Ciamician", Alma Mater Studiorum, 40126 Bologna, Italy*

Roberta De Ventura − *Dipartimento di Chimica "Giacomo Ciamician", Alma Mater Studiorum, 40126 Bologna, Italy*

Marianna Marchini − *Dipartimento di Chimica "Giacomo Ciamician", Alma Mater Studiorum, 40126 Bologna, Italy;* orcid.org/0000-0002-9746-2062

Paola Ceroni − *Dipartimento di Chimica "Giacomo Ciamician", Alma Mater Studiorum, 40126 Bologna, Italy;* orcid.org/0000-0001-8916-1473

Carlos Silva López − *Departamento de Química Orgánica, Universidad de Vigo, 36310 Vigo, Spain;* orcid.org/0000-0003-4955-9844

Complete contact information is available at: https://pubs.acs.org/10.1021/acsorginorgau.1c00052

Notes

The authors declare no competing financial interest.

■ ACKNOWLEDGMENTS

Acknowledgements are made to University of Bologna for financial support. M.B. is also grateful to the PRIN-2017 project 2017W8KNZW for financial support. C.S.L. is grateful to the Ministerio de Ciencia for financial support (PID2020-115789GB-C22) and CESGA for allocation of HPC time.

■ REFERENCES

(1) Mato, M.; Franchino, A.; García-Morales, C.; Echavarren, A. M. Gold-Catalyzed Synthesis of Small Rings. *Chem. Rev.* **2021**, *121*, 8613−8684.

(2) Wang, T.; Hashmi, A. S. K. 1,2-Migrations onto Gold Carbene Centers. *Chem. Rev.* **2021**, *121*, 8948−8978.

(3) Campeau, D.; Leon Rayo, D. F.; Mansour, A.; Muratov, K.; Gagosz, F. Gold-Catalyzed Reactions of Specially Activated Alkynes, Allenes, and Alkenes. *Chem. Rev.* **2021**, *121*, 8756−8867.

(4) Rocchigiani, L.; Bochmann, M. Recent Advances in Gold(III) Chemistry: Structure, Bonding, Reactivity, and Role in Homogeneous Catalysis. *Chem. Rev.* **2021**, *121*, 8364−8451.

(5) Hashmi, A. S. K. Dual Gold Catalysis. *Acc. Chem. Res.* **2014**, *47*, 864−876.

(6) Pflästerer, D.; Hashmi, A. S. K. Gold catalysis in total synthesis − recent achievements. *Chem. Soc. Rev.* **2016**, *45*, 1331−1367.

(7) Zeitler, K.; Neumann, M. Synergistic visible light photoredox catalysis. *Phys. Sci. Rev.* **2019**, *5*, 20170173.

(8) Nijamudheen, A.; Datta, A. Gold-Catalyzed Cross-Coupling Reactions: An Overview of Design Strategies, Mechanistic Studies, and Applications. *Chem. Eur. J.* **2020**, *26*, 1442−1487.

(9) Zuccarello, G.; Escofet, I.; Caniparoli, U.; Echavarren, A. M. New-Generation Ligand Design for the Gold-Catalyzed Asymmetric Activation of Alkynes. *ChemPlusChem.* **2021**, *86*, 1283−1296.

(10) Díez-González, S.; Marion, N.; Nolan, S. P. N-Heterocyclic Carbenes in Late Transition Metal Catalysis. *Chem. Rev.* **2009**, *109*, 3612−3676.

(11) Hopkinson, M. N.; Richter, C.; Schedler, M.; Glorius, F. An overview of N-heterocyclic carbenes. *Nature* **2014**, *510*, 485−496.

(12) Zhang, D.; Zi, G. N-heterocyclic carbene (NHC) complexes of group 4 transition metals. *Chem. Soc. Rev.* **2015**, *44*, 1898−1921.

(13) Peris, E. Smart N-Heterocyclic Carbene Ligands in Catalysis. *Chem. Rev.* **2018**, *118*, 9988−10031.

(14) Marion, N.; Nolan, S. P. N-Heterocyclic carbenes in gold catalysis. *Chem. Soc. Rev.* **2008**, *37*, 1776−1782.

(15) Nolan, S. P. The Development and Catalytic Uses of N-Heterocyclic Carbene Gold Complexes. *Acc. Chem. Res.* **2011**, *44*, 91−100.

(16) Gatineau, D.; Goddard, J.-P.; Mouriès-Mansuy, V.; Fensterbank, L. When NHC Ligands Make a Difference in Gold. *Catalysis, Isr. J. Chem.* **2013**, *53*, 892−900.

(17) Tang, X.-T.; Yang, F.; Zhang, T.-T.; Liu, Y.-F.; Liu, S.-Y.; Su, T.-F.; Lv, D.-C.; Shen, W.-B. Recent Progress in N-Heterocyclic Carbene Gold-Catalyzed Reactions of Alkynes Involving Oxidation/Amination/Cycloaddition. *Catalysts* **2020**, *10*, 350.

(18) Nahra, F.; Tzouras, N. V.; Collado, A.; Nolan, S. P. Synthesis of N-heterocyclic carbene gold(I) complexes. *Nat. Prot.* **2021**, *16*, 1476−1493.

(19) Wang, Y.; Muratore, M. E.; Echavarren, A. M. Gold Carbene or Carbenoid: Is There a Difference? *Chem. Eur. J.* **2015**, *21*, 7332−7339.

(20) Muñoz-Castro, A.; Carey, D. M.; Arratia-Perez, R. Relativistic effects on dative carbon-coinage metal bond. Evaluation of NHC-MCl (M = Cu, Ag, Au) from relativistic DFT. *Polyhedron* **2021**, *197*, 115020.

(21) Zargaran, P.; Wurm, T.; Zahner, D.; Schießl, J.; Rudolph, M.; Rominger, F.; Hashmi, A. S. K. A Structure-Based Activity Study of

Highly Active Unsymmetrically Substituted NHC Gold(I) Catalysts. *Adv.Synth.Catal.* **2018**, *360*, 106−111.
(22) Wurm, T.; Hornung, J.; O'Neill, M.; Rudolph, M.; Rominger, F.; Hashmi, A. S. K. Synthesis of Ester- and Phosphonate-Functionalized Au^{I}−Imidazolylidene Chlorides through the Isonitrile Route. *Chem. Eur. J.* **2017**, *23*, 5143−5147.
(23) Kong, L.; Morvan, J.; Pichon, D.; Jean, M.; Albalat, M.; Vives, T.; Colombel-Rouen, S.; Giorgi, M.; Dorcet, V.; Roisnel, T.; Crévisy, C.; Nuel, D.; Nava, P.; Humbel, S.; Vanthuyne, N.; Mauduit, M.; Clavier, H. From Prochiral N-Heterocyclic Carbenes to Optically Pure Metal Complexes: New Opportunities in Asymmetric Catalysis. *J. Am. Chem. Soc.* **2020**, *142*, 93−98.
(24) Alcarazo, M.; Roseblade, S. J.; Cowley, A. R.; Fernández, R.; Brown, J. M.; Lassaletta, J. M. A Versatile Architecture for Stable N-Heterocyclic Carbenes. *J. Am. Chem. Soc.* **2005**, *127*, 3290−3291.
(25) Burstein, C.; Lehmann, C. W.; Glorius, F. Imidazo[1,5-a]pyridine-3-ylidenes—pyridine derived N-heterocyclic carbene ligands. *Tetrahedron* **2005**, *61*, 6207−6217.
(26) Roseblade, R. J.; Ros, A.; Monge, D.; Alcarazo, M.; Álvarez, E.; Lassaletta, J. M.; Fernández, R. Imidazo[1,5-a]pyridin-3-ylidene/Thioether Mixed C/S Ligands and Complexes Thereof. *Organometallics* **2007**, *26*, 2570−2578.
(27) Fürstner, A.; Alcarazo, M.; Krause, H.; Lehmann, C. W. Effective Modulation of the Donor Properties of N-Heterocyclic Carbene Ligands by "Through-Space" Communication within a Planar Chiral Scaffold. *J. Am. Chem. Soc.* **2007**, *129*, 12676−12677.
(28) Nakano, R.; Nozaki, K. Copolymerization of Propylene and Polar Monomers Using Pd/IzQO Catalysts. *J. Am. Chem. Soc.* **2015**, *137*, 10934−10937.
(29) Iglesias-Sigüenza, J.; Izquierdo, C.; Diez, E.; Fernández, R.; Lassaletta, J. M. Chirality and catalysis with aromatic N-fused heterobicyclic carbenes. *Dalton Trans.* **2016**, *45*, 10113−10117.
(30) Park, D.-A.; Ryu, J. Y.; Lee, J.; Hong, S. Bifunctional N-heterocyclic carbene ligands for Cu-catalyzed direct C−H carboxylation with CO2. *RSC Adv.* **2017**, *7*, 52496−52502.
(31) Tao, W.; Akita, S.; Nakano, R.; Ito, S.; Hoshimoto, Y.; Ogoshi, S.; Nozaki, K. Copolymerisation of ethylene with polar monomers by using palladium catalysts bearing an N-heterocyclic carbene-phosphine oxide bidentate ligand. *Chem. Commun.* **2017**, *53*, 2630−2633.
(32) Byun, S.; Seo, H.; Choi, J.-H.; Ryu, J. Y.; Lee, J.; Chung, W.-J.; Hong, S. Fluoro-imidazopyridinylidene Ruthenium Catalysts for Cross Metathesis with Ethylene. *Organometallics* **2019**, *38*, 4121−4132.
(33) Chen, K.; Chen, W.; Yi, X.; Chen, W.; Liu, M.; Wu, H. Sterically hindered N-heterocyclic carbene/palladium(ii) catalyzed Suzuki−Miyaura coupling of nitrobenzenes. *Chem. Commun.* **2019**, *55*, 9287−9290.
(34) Kriechbaum, M.; List, M.; Berger, R. J. F.; Patzschke, M.; Monkowius, U. Silver and Gold Complexes with a New 1,10-Phenanthroline Analogue N-Heterocyclic Carbene: A Combined Structural, Theoretical, and Photophysical Study. *Chem. Eur. J.* **2012**, *18*, 5506−5509.
(35) Espina, M.; Rivilla, I.; Conde, A.; Díaz-Requejo, M. M.; Pérez, P. J.; Álvarez, E.; Fernández, R.; Lassaletta, J. M. Chiral, Sterically Demanding N-Heterocyclic Carbenes Fused into a Heterobiaryl Skeleton: Design, Synthesis, and Structural Analysis. *Organometallics* **2015**, *34*, 1328−1338.
(36) Grande-Carmona, F.; Iglesias-Sigüenza, J.; Álvarez, E.; Díez, E.; Fernández, R.; Lassaletta, J. M. Synthesis and Characterization of Axially Chiral Imidazoisoquinolin-2-ylidene Silver and Gold Complexes. *Organometallics* **2015**, *34*, 5073−5080.
(37) Rana, B. K.; Nandy, A.; Bertolasi, V.; Bielawski, C. W.; Das Saha, K.; Dinda, J. Novel Gold(I)− and Gold(III)−N-Heterocyclic Carbene Complexes: Synthesis and Evaluation of Their Anticancer Properties. *Organometallics* **2014**, *33*, 2544−2548.
(38) Francos, J.; Grande-Carmona, F.; Faustino, H.; Iglesias-Sigüenza, J.; Díez, E.; Alonso, I.; Fernández, R.; Lassaletta, J. M.; López, F.; Mascareñas, J. L. Axially Chiral Triazoloisoquinolin-3-ylidene Ligands in Gold(I)-Catalyzed Asymmetric Intermolecular (4 + 2) Cycloadditions of Allenamides and Dienes. *J. Am. Chem. Soc.* **2012**, *134*, 14322−14325.
(39) Varela, I.; Faustino, H.; Díez, E.; Iglesias-Sigüenza, J.; Grande-Carmona, F.; Fernández, R.; Lassaletta, J. M.; Mascareñas, J. L.; López, F. Gold(I)-Catalyzed Enantioselective [2 + 2+2] Cycloadditions: An Expedient Entry to Enantioenriched Tetrahydropyran Scaffolds. *ACS Catal.* **2017**, *7*, 2397−2402.
(40) Zhang, J.-Q.; Liu, Y.; Wang, X.-W.; Zhang, L. Synthesis of Chiral Bifunctional NHC Ligands and Survey of Their Utilities in Asymmetric Gold Catalysis. *Organometallics* **2019**, *38*, 3931−3938.
(41) Tang, Y.; Benaissa, I.; Huynh, M.; Vendier, L.; Lugan, N.; Bastin, S.; Belmont, P.; César, V.; Michelet, V. An Original L-shape, Tunable N-Heterocyclic Carbene Platform for Efficient Gold(I) Catalysis. *Angew. Chem., Int. Ed.* **2019**, *58*, 7977−7981.
(42) Kim, Y.; Kim, Y.; Hur, M. Y.; Lee, E. Efficient synthesis of bulky N-Heterocyclic carbene ligands for coinage metal complexes. *J. Organomet. Chem.* **2016**, *820*, 1−7.
(43) Cera, G.; Chiarucci, M.; Mazzanti, A.; Mancinelli, M.; Bandini, M. Enantioselective Gold-Catalyzed Synthesis of Polycyclic Indolines. *Org. Lett.* **2012**, *14*, 1350−1353.
(44) Chiarucci, M.; di Lillo, M.; Romaniello, A.; Cozzi, P. G.; Cera, G.; Bandini, M. Gold meets enamine catalysis in the enantioselective α-allylic alkylation of aldehydes with alcohols. *Chem. Sci.* **2012**, *3*, 2859−2863.
(45) Cera, G.; Piscitelli, S.; Chiarucci, M.; Fabrizi, G.; Goggiamani, A.; Ramón, R. S.; Nolan, S. P.; Bandini, M. One-Pot Gold-Catalyzed Synthesis of Azepino[1,2-a]indoles. *Angew. Chem., Int. Ed.* **2012**, *51*, 9891−9895.
(46) Chiarucci, M.; Mocci, R.; Syntrivanis, L.-D.; Cera, G.; Mazzanti, A.; Bandini, M. Merging Synthesis and Enantioselective Functionalization of Indoles by a Gold-Catalyzed Asymmetric Cascade Reaction. *Angew. Chem., Int. Ed.* **2013**, *52*, 10850−10853.
(47) Jia, M.; Monari, M.; Yang, Q.-Q.; Bandini, M. Enantioselective gold catalyzed dearomative [2 + 2]-cycloaddition between indoles and allenamides. *Chem. Commun.* **2015**, *51*, 2320−2323.
(48) Mastandrea, M. M.; Mellonie, N.; Giacinto, P.; Collado, A.; Nolan, S. P.; Miscione, G. P.; Bottoni, A.; Bandini, M. Gold(I)-Assisted α-Allylation of Enals and Enones with Alcohols. *Angew. Chem. Int. Ed.* **2015**, *54*, 14885−14889.
(49) An, J.; Parodi, A.; Monari, M.; Reis, M. C.; Lopez, C. S.; Bandini, M. Gold-Catalyzed Dearomatization of 2-Naphthols with Alkynes. *Chem Eur. J.* **2017**, *23*, 17473−17477.
(50) An, J.; Pedrazzani, R.; Monari, M.; Marin-Luna, M.; Lopez, C. S.; Bandini, M. Site-selective synthesis of 1,3-dioxin-3-ones via a gold(I) catalyzed cascade reaction. *Chem. Commun.* **2020**, *56*, 7734−7737.
(51) Albano, V. G.; Bandini, M.; Melucci, M.; Monari, M.; Piccinelli, F.; Tommasi, S.; Umani-Ronchi, A. Novel Chiral Diamino-Oligothiophenes as Valuable Ligands in Pd-Catalyzed Allylic Alkylations. On the "Primary" Role of "Secondary" Interactions in Asymmetric Catalysis. *Adv. Synth. Catal.* **2005**, *347*, 1507−1512.
(52) Melucci, M.; Gazzano, M.; Barbarella, G.; Cavallini, M.; Biscarini, F.; Piccinelli, F.; Monari, M.; Bandini, M.; Bongini, A.; Umani-Ronchi, A.; Biscarini, P. Synthesis, Multiphase Characterization, and Helicity Control in Chiral DACH-Linked Oligothiophenes. *Chem. Eur. J.* **2006**, *12*, 7304−7312.
(53) Albano, V. G.; Bandini, M.; Monari, M.; Tommasi, S.; Piccinelli, F.; Umani-Ronchi, A. Synthesis, structural characterization, and catalytic activity of chiral diamine and diimine Pd(II)-complexes. *Inorg. Chim. Acta* **2007**, *360*, 1000−1008.
(54) Bandini, M.; Eichholzer, A.; Tommasi, S.; Umani-Ronchi, A. Practical Aspects in the Gram-Scale Synthesis of Chiral Diamino-Bithiophene 'DAT2' Ligand. *Synthesis* **2007**, *2007*, 1587−1588.
(55) Albano, V. G.; Bandini, M.; Moorlag, C.; Piccinelli, F.; Pietrangelo, A.; Tommasi, S.; Umani-Ronchi, A.; Wolf, M. O. Electropolymerized Pd-Containing Thiophene Polymer: A Reusable Supported Catalyst for Cross-Coupling Reactions. *Organometallics* **2007**, *26*, 4373−4375.

https://doi.org/10.1021/acsorginorgau.1c00052
ACS Org. Inorg. Au 2022, 2, 229−235

(56) Bandini, M.; Melucci, M.; Piccinelli, F.; Sinisi, R.; Tommasi, S.; Umani-Ronchi, A. New chiral diamino-bis(tert-thiophene): an effective ligand for Pd- and Zn-catalyzed asymmetric transformations. *Chem. Commun.* **2007**, 4519−4521.
(57) Schmidbaur, H.; Schier, A. Gold η^2-Coordination to Unsaturated and Aromatic Hydrocarbons: The Key Step in Gold-Catalyzed Organic Transformations. *Organometallics* **2010**, *29*, 2−23.
(58) Ni, Q.-L.; Jiang, X.-F.; Huang, T.-H.; Wang, X.-J.; Gui, L.-C.; Yang, K.-G. Gold(I) Chloride Complexes of Polyphosphine Ligands with Electron-Rich Arene Spacer: Gold−Arene Interactions. *Organometallics* **2012**, *31*, 2343−2348.
(59) An, J.; Lombardi, L.; Grilli, S.; Bandini, M. PPh_3AuTFA Catalyzed in the Dearomatization of 2-Naphthols with Allenamides. *Org. Lett.* **2018**, *20*, 7380−7383.
(60) Pedrazzani, R.; An, J.; Monari, M.; Bandini, M. New Chiral BINOL-Based Phosphates for Enantioselective [Au(I)]-Catalyzed Dearomatization of β-Naphthols with Allenamides. *Eur. J. Org. Chem.* **2021**, *2021*, 1732−1736.
(61) Zhuo, C.-X.; Zhang, W.; You, S.-L. Catalytic Asymmetric Dearomatization Reactions. *Angew. Chem., Int. Ed. Engl.* **2012**, *51*, 12662−12686.
(62) Zheng, C.; You, S.-L. Catalytic Asymmetric Dearomatization by Transition-Metal Catalysis: A Method for Transformations of Aromatic Compounds. *Chem.* **2016**, *1*, 830−857.
(63) You, S.-L. *Asymmetric Dearomatization Reactions*; Wiley-VCH, 2016. (f) Wu, W.-T.; Zhang, L.; You, S.-L. Catalytic asymmetric dearomatization (CADA) reactions of phenol and aniline derivatives. *Chem. Soc. Rev.* **2016**, *45*, 1570−1580.
(64) Wu, W.-T.; Zhang, L.; You, S.-L. Recent Progress on Gold-catalyzed Dearomatization Reactions. *Acta Chim. Sinica* **2017**, *75*, 419−438.
(65) An, J.; Bandini, M. Gold-catalyzed Dearomatization Reactions. *CHIMIA* **2018**, *72*, 610−613.
(66) Xia, Z.-L.; Xu-Xu, Q.-F.; Zheng, C.; You, S.-L. Chiral phosphoric acid-catalyzed asymmetric dearomatization reactions. *Chem. Soc. Rev.* **2020**, *49*, 286−300.
(67) An, J.; Bandini, M. Recent Advances in the Catalytic Dearomatization of Naphthols. *Eur. J. Org. Chem.* **2020**, *2020*, 4087−4097.
(68) Lu, T.; Lu, Z. J.; Ma, Z. X.; Zhang, Y.; Hsung, R. P. Allenamides: A Powerful and Versatile Building Block in Organic Synthesis. *Chem. Rev.* **2013**, *113*, 4862−4904.
(69) Manoni, E.; Bandini, M. N-Allenyl Amides and O-Allenyl Ethers in Enantioselective Catalysis. *Eur. J. Org. Chem.* **2016**, *2016*, 3135−3142.
(70) Li, X.; Liu, Y.; Ding, N.; Tan, X.; Zhao, Z. Recent progress in transition-metal-free functionalization of allenamides. *RSC Adv.* **2020**, *10*, 36818−36827.
(71) Herrero-Gómez, E.; Nieto-Oberhuber, C.; López, S.; Benet-Buchholz, J.; Echavarren, A. M. Cationic $\eta1/\eta2$-Gold(I) Complexes of Simple Arenes. *Angew. Chem., Int. Ed.* **2006**, *45*, 5455−5459.
(72) Touil, M.; Bechem, B.; Hashmi, A. S. K.; Engels, B.; Omary, M. A.; Rabaâ, H. Theoretical study of weak CC double bond coordination in a gold (I) catalyst precursor. *J. Mol. Struct.: THEOCHEM* **2010**, *957*, 21−25.
(73) The partial effectiveness of IPrAuCl/AgTFA (5 mol%) in promoting the dearomatization of **12** with **13** was already proven (55% yield, see ref 75). On the contrary, dinuclear $[\{Au(IPr)\}_2(\mu\text{-}OH)][BF_4]$ (see ref 18 and references therein) proved inefficient in the present model dearomatization reaction.
(74) Caracelli, I.; Zukerman-Schpector, J.; Tiekink, E. R. T. Supramolecular synthons based on gold···π(arene) interactions. *Gold Bull.* **2013**, *46*, 81−89.
(75) Christian, A. H.; Niemeyer, Z. L.; Sigman, M. S.; Toste, F. D. Uncovering Subtle Ligand Effects of Phosphines Using Gold(I) Catalysis. *ACS Catal.* **2017**, *7*, 3973−3978.
(76) Ham, J. H.; Cho, J.; Nayab, S.; Jeong, J. H. Synthesis and structural characterisation of copper complexes containing methylthiophene and methylfuryl derivatives of (*R*,*R*)-1,2-diaminocyclohexane as precatalysts for polymerisation of *rac*-lactide. *Inorg. Chim. Acta* **2018**, *480*, 33−41.
(77) Veracini, A. A.; Macciantelli, D.; Lunazzi, L. Conformational analysis of bithienyl derivatives: a liquid crystal nuclear magnetic resonance approach. *J. Chem. Soc., Perkin Trans.* **1973**, *2*, 751−754.
(78) Tsuzuki, S.; Orita, H.; Sato, N. Intermolecular interactions of oligothienoacenes: Do S···S interactions positively contribute to crystal structures of sulfur-containing aromatic molecules? *J. Chem. Phys.* **2016**, *145*, 174503.
(79) We might speculate that the *cis*-thienyl conformations could also be present in the solution, with a consequent overall modification of both steric cage of the gold complex as well as electronic interactions of the thienyl sulfur atoms with the Au center during the reaction course.
(80) Hohenberg, P.; Kohn, W. Inhomogeneous Electron Gas. *Phys. Rev.* **1964**, *136*, B864.
(81) Kohn, W.; Sham, L. J. Self-Consistent Equations Including Exchange and Correlation Effects. *Phys. Rev.* **1965**, *140*, A1133.
(82) Bader, R. F. W.; Popelier, P. L. A.; Keith, T. A. Theoretical Definition of a Functional Group and the Molecular Orbital Paradigm. *Angew. Chem., Int. Ed.* **1994**, *33*, 620.
(83) Contreras-García, J.; Johnson, E. R.; Keinan, S.; Chaudret, R.; Piquemal, J.-P.; Beratan, D. N.; Yang, W. A Program for Plotting Noncovalent Interaction Regions. *J. Chem. Theory Comput.* **2011**, *7*, 625−632.
(84) Becke, A. D. Density-functional exchange-energy approximation with correct asymptotic-behavior. *Phys. Rev. A* **1988**, *38*, 3098.
(85) Lee, C.; Yang, W.; Parr, R. G. Development of the Colle-Salvetti correlation-energy formula into a functional of the electron density. *Phys. Rev. B* **1988**, *37*, 785.
(86) Faza, O. N.; Rodríguez, R. A.; López, C. S. Performance of density functional theory on homogeneous gold catalysis. *Theor. Chem. Acc.* **2011**, *128*, 647−661.
(87) Faza, O. N.; López, C. S. Computational Approaches to Homogeneous Gold Catalysis. *Top. Curr. Chem.* **2014**, *357*, 213−284.
(88) Johansson, M. J.; Gorin, D. J.; Staben, S. T.; Toste, F. D. Gold(I)-Catalyzed Stereoselective Olefin Cyclopropanation. *J. Am. Chem. Soc.* **2005**, *127*, 18002−18003.
(89) Handa, S.; Slaughter, L. M. Enantioselective Alkynylbenzaldehyde Cyclizations Catalyzed by Chiral Gold(I) Acyclic Diaminocarbene Complexes Containing Weak Au−Arene Interactions. *Angew. Chem., Int. Ed.* **2012**, *51*, 2912−2915.
(90) The cyclopropanation and the alkynylbenzaldehyde cyclization were also carried out in the presence of a 2.5 mol% catalyst loading. In these cases, a marked accelerating effect with **10c** was also observed: cyclopropanation, **10a** yield = 50%, **10c** yield = 62%, **10d** yield = 38%; alkynylbenzaldehyde, **10a** yield = 32%, **10c** yield = 45%, **10d** yield = 17%.

https://doi.org/10.1021/acsorginorgau.1c00052
ACS Org. Inorg. Au 2022, 2, 229−235